Journal of Molecular Structure 1102 (2015) 267–274

Contents lists available at ScienceDirect

Journal of Molecular Structure

journal homepage: http://www.elsevier.com/locate/molstruc

Raman, IR and DFT studies of mechanism of sodium binding to urea catalyst

Partha P. Kundu [a, 1, 2], Gayatri Kumari [a, 1], Arjun K. Chittoory [b, 1], Sridhar Rajaram [c, 1], Chandrabhas Narayana [a, 1, *]

[a] Chemistry and Physics of Materials Unit, Jawaharlal Nehru Centre for Advanced Scientific Research, Bangalore, India
[b] New Chemistry Unit, Jawaharlal Nehru Centre for Advanced Scientific Research, Bangalore, India
[c] International Centre for Materials Science, Jawaharlal Nehru Centre for Advanced Scientific Research, Bangalore, India

ARTICLE INFO

Article history:
Received 18 April 2015
Received in revised form
5 July 2015
Accepted 12 August 2015
Available online 7 September 2015

Keywords:
IR and Raman spectroscopy
DFT
NBO
Sulfonyl urea
Hydrogen-bonding catalyst
Conformational change

ABSTRACT

Bis-camphorsulfonyl urea, a newly developed hydrogen bonding catalyst, was evaluated in an enantioselective Friedel–Crafts reaction. We observed that complexation of the sulfonyl urea with a sodium cation enhanced the selectivity of reactions in comparison to reactions performed with urea alone. To understand the role of sodium cation, we performed Infrared and Raman spectroscopic studies. The detailed band assignment of the molecule was made by calculating spectra using Density Functional theory. Our studies suggest that the binding of the cation takes place through the oxygen atoms of carbonyl and sulfonyl groups. Natural Bond Orbital (NBO) analysis shows the expected charge distribution after sodium binding. The changes in the geometrical parameter and charge distribution are in line with the experimentally observed spectral changes. Based on these studies, we conclude that binding of the sodium cation changes the conformation of the sulfonyl urea to bring the chiral camphor groups closer to the incipient chiral center.

1. Introduction

Hydrogen-bond catalysis has been developed as a benign alternative to Lewis acid catalyzed reactions. In these systems, activation of substrates is accomplished by formation of hydrogen bonds between the catalyst and Lewis basic sites on the reactants [1–7]. The acidity of the hydrogen bond donor plays an important role in determining the turn over frequency and selectivity of the reaction [8–10].

We recently reported the development of a novel bis-camphorsulfonyl urea as a highly acidic hydrogen bond catalyst [11]. To evaluate this catalyst, we used it in a well studied Friedel–Crafts reaction of nitroalkenes [12–19]. The enantioselectivity of this reaction turned out to be strongly dependent on the presence of $NaBPh_4$ as an additive. Addition of $NaBPh_4$, a weak Lewis acid, changed the face selection and enhanced the enantioselectivity (see Scheme 1, Panel B) [11]. We found that addition of other alkali metal salts did not change the face selection or improve enantioselectivity. In the case of a more Lewis acidic magnesium salt, a rapid background reaction was observed. We hypothesized that the $NaBPh_4$ was binding the Lewis basic sites on the catalyst and effecting a change in the conformation (see Scheme 1, panel A) that lead to the enhancement in selectivity. In order to understand the role of $NaBPh_4$ in this reaction, we prepared the complex and studied the structure of the complex using IR and Raman spectroscopy. A correct interpretation of the spectra requires a thorough theoretical determination of the band assignments. Apart from this, the calculations should also accurately reflect the changes in frequencies observed upon sodium binding. These changes can be attributed to the change in geometrical parameters and charge distribution as seen in our calculations. Herein we report on the results of our calculation that clearly shows the change in conformation of our catalytic system upon sodium binding which facilitates enantioselectivity.

2. Methods

2.1. Experimental section

All Raman measurements were performed in the 180°

* Corresponding author.
E-mail address: cbhas@jncasr.ac.in (C. Narayana).
[1] http:www.jncasr.ac.in.
[2] Current address: Department of Physics, M.S. Ramaiah University of Applied Sciences, Bengaluru, 560058 India.

http://dx.doi.org/10.1016/j.molstruc.2015.08.029
0022-2860/

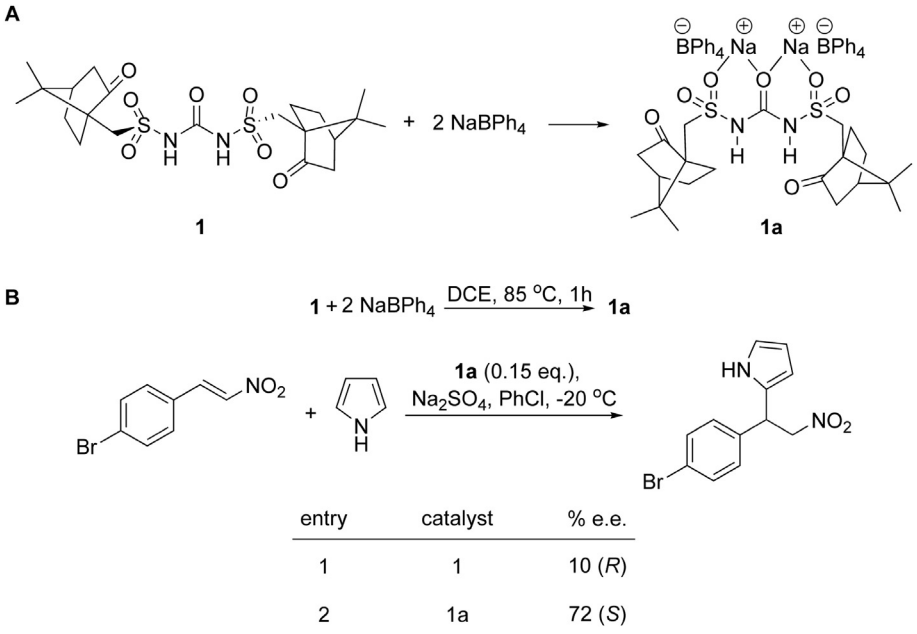

entry	catalyst	% e.e.
1	1	10 (*R*)
2	1a	72 (*S*)

Scheme 1. (A) Proposed change in conformation due to sodium binding. (B) Change in selectivity with sodium binding.

backscattering geometry, using diode pumped frequency doubled Nd:YAG (model GDLM-5015 L, Photop Suwtech Inc., China) solid state laser as an excitation source. The spectrometer comprises of SPEX TRIAX 550 monochromator and a liquid nitrogen cooled charge-coupled device (CCD; Spectrum One with CCD 3000 controller, ISA Jobin Yvon). A holographic 1800 grooves mm^{-1} grating was used along with the 200 μm spectrograph entrance slit setting, providing ~2 cm^{-1} resolution. A 50 × infinity-corrected objective (Nikon LPlan, Japan, NA 0.45) was used. The laser power used at the sample was 2 mW and the typical accumulation time was 180s. The details of this custom build Raman spectrometer is given elsewhere [20]. All spectra were background corrected and smoothed by 5 point FFT filter technique using Origin software. Lorentzian-profiles were fitted for spectral analysis. IR spectra were recorded on a Bruker IFS 66v/S spectrophotometer with KBr pellets containing the sample in the region 400–4000 cm^{-1}. Background was subtracted using OPUS software.

2.2. Computational methods

All quantum chemical calculations have been performed at the density functional theory (DFT) level as employed in Gaussian 09 (G09) suite of program [21]. In order to take into account the effect of the intermolecular interaction present in solid state, we have considered a dimer of the catalyst. The initial orientation of the dimer was taken from the crystal structure and subsequently geometry optimization was performed using Becke three-parameter hybrid-exchange functional [22] and Lee, Yang and Parr (B3LYP) gradient corrected correlation functional [23]. 6-31G (d,p) basis set was employed for such calculation. Harmonic vibrational frequencies were calculated on the optimized geometry using the same level of theory. The absence of any negative frequency confirms that the geometry corresponds to the local minimum at the potential energy surface. In order to compare the spectral change of the catalyst upon Na^+ binding, we considered monomer of the solid urea catalyst. Catalyst in its free and bound form were optimized with the same level of theory mentioned above. In all the cases, a dual scaling factor was used for the calculated vibrational frequencies. Frequencies below 1000 cm^{-1} were not scaled, whereas those above 1000 cm^{-1} were scaled with 0.961 [24]. The output of the Gaussian provide the Raman activities. In order to match with the experimental spectra, these are converted to Raman intensity [25–27]. The potential energy distribution (PED) calculation was performed by VEDA program [28]. Natural Bond Orbital (NBO) calculation has been carried out by NBO 3.1 program [29].

3. Results and discussion

3.1. Vibrational assignments

We initially performed calculations on the monomer and found that the intensity profile did not match well with the experimentally obtained spectrum. This clearly indicates that neighboring molecules impact vibrational frequencies. In order to partially account for this effect, we have performed our calculations on the dimer of the catalyst. The optimized dimer of the urea catalyst is shown in Fig. 1. The experimental and simulated IR and Raman spectra are shown in Figs. 2 and 3, respectively. The detailed assignment of the IR and Raman bands are given in SI. Herein, we restrict our discussion to bands that show maximal sensitivity to Na^+ binding.

Carbonyl groups are present in different classes of organic compounds and have all the characteristics required for producing good group frequency. They give rise to a strong band in IR owing to their large dipole moment derivative. Since they have a large force constant, >*C*=*O* stretching frequency appears out of the fingerprint region and does not overlap with other modes. In organic compounds, carbonyl groups are generally bonded with groups that have lower frequency. This mismatch weakens the mechanical coupling, yielding almost a pure mode in the range 1750 ± 150 cm^{-1} [30]. This mode is sensitive to the local environment, and provides additional information about the carbonyl's surroundings. Our compound has two types of carbonyl groups,viz., a keto carbonyl on the camphor ring and a urea carbonyl. It is important to distinguish their contribution in the spectrum. The position of these bands is governed by a number of factors such as mass of the adjacent atoms, their electronegativity, geometry and electronic structure (resonance and inductive effects) [30]. As these

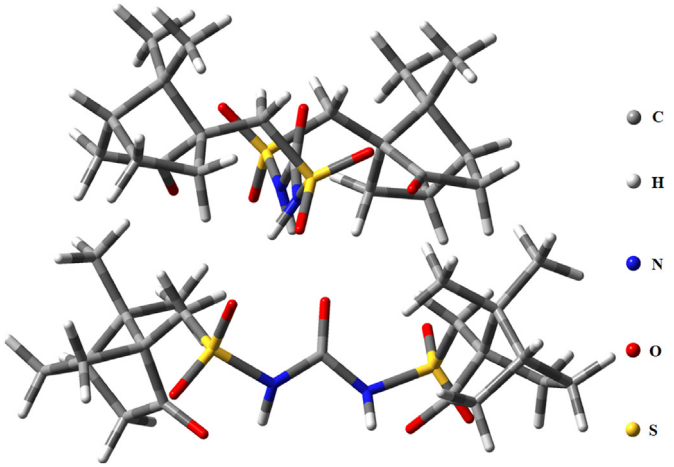

Fig. 1. The optimized structure of urea catalyst in the dimer form.

factors may compete with each other, determining the position of such bands is non-trivial and requires theoretical calculation. In the IR spectrum of sulfonyl area, we observe two strong bands at 1734 and 1747 cm^{-1} which are assigned to carbonyl stretching of camphor group. Theoretically predicted values of these modes are 1748 and 1768 cm^{-1}. In Raman, the contribution from camphor carbonyl appears at 1754 cm^{-1} as a medium band and the corresponding theoretical value is 1768 cm^{-1}. Assignment of these bands is further confirmed by literature precedence [31,32]. The band of medium intensity at 1706 cm^{-1} in the IR spectrum is ascribed to >*C*=*O* stretching of urea carbonyl, while its theoretically predicted value is 1698 cm^{-1}. In Raman spectrum, we see bands at 1709 and 1728 cm^{-1}, which are assigned to stretching of the urea carbonyl. Our assignment is confirmed by DFT calculations that show the corresponding bands at 1698 and 1722 cm^{-1}. For similar compounds >*C*=*O* vibration has been reported to be around 1700 cm^{-1} [33,34]. All these modes are almost pure (contribution of 80% or more in PED) as expected. Thus we distinguished two different >*C*=*O* stretches with our calculations.

The antisymmetric and symmetric stretching modes of SO_2 appear in the ranges of 1300–1360 and 1130–1190 cm^{-1}, respectively [35]. Their exact positions depend on the electro-negativity of the groups attached to them [36]. In IR these bands are very strong, while their intensity varies considerably in Raman [30]. In our compound, two strong bands at 1139 and 1344 cm^{-1} are observed in IR, and these are assigned to $\nu_s(SO_2)$ and $\nu_{as}(SO_2)$. The calculated modes for these vibrations appear at 1068 and 1293 cm^{-1} respectively. The PED calculation shows that these modes are not pure and have contribution from other groups. Based on our PED calculation we also observe two modes at 1139 and 1282 cm^{-1} which have small contribution from antisymmetric and symmetric stretching of SO_2. Theoretical values for these modes are at 1083 and 1249 cm^{-1} respectively. In Raman spectrum, a medium band at 1299 cm^{-1} and a weak band at 1112 cm^{-1} are assigned to the antisymmetric and symmetric stretching of SO_2, respectively. The corresponding theoretically predicted values are 1249 and 1068 cm^{-1}. In earlier reports, SO_2 stretching vibrations have been reported at 1314, 1308, 1274, 1157, 1147 and 1133 cm^{-1} by Hangan et al. [37], while Chohan and co-workers [38] have reported values of 1110 and 1345 cm^{-1}.

The C–N stretching mode appears as a medium band at 1200 cm^{-1} in IR. In our DFT calculation this mode appears at 1170 cm^{-1}. PED calculation suggests that this mode mixes with other modes. Assignment of this vibration was also confirmed from literature [39–43].

Two broad bands at 3268 and 3169 cm^{-1} in IR are attributed to the N–H stretching of secondary amide. This is in good agreement with the literature [44,45,33]. PED calculation indicates that these modes are almost pure.

3.2. Effect of Na^+ binding on the optimized geometry

In order to understand the effect of Na^+ on the conformation of the catalyst, we added two Na^+ ions close to the oxygens of the carbonyl and sulfonyl groups in the monomeric form of the urea. We then performed geometry optimization (Fig. 4). The numbering of atoms is shown in Fig. 4. Table 1 summarizes the selected geometrical parameters of the catalyst in the free and Na^+ bound form.

As can be seen in Table 1, >*C*=*O* bond length of urea carbonyl increased (0.0328 Å) upon Na^+ binding. Metal binding shortened

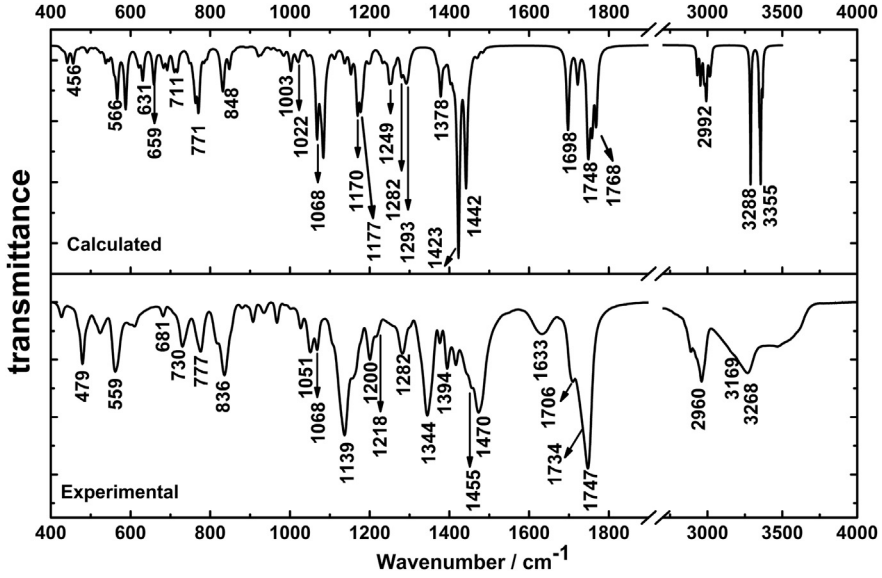

Fig. 2. The experimental and theoretically calculated IR spectra of urea catalyst.

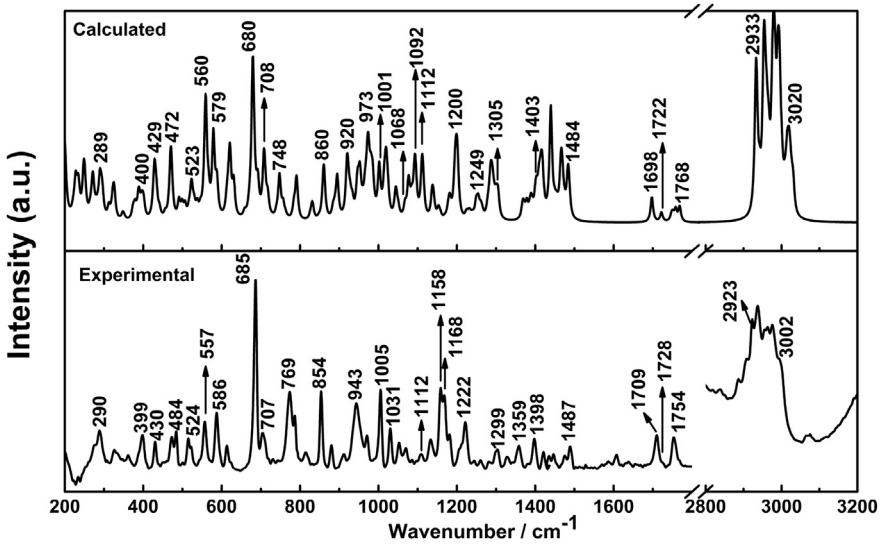

Fig. 3. The experimental and theoretically calculated Raman spectra of urea catalyst.

both the C–N bonds (0.012–0.015 Å) while the bond length of the two N–H bonds increased (~0.012 Å). Na^+ binding to the catalyst causes the two sulfonyl groups to become equivalent. Apart from this, the S=O bond lengths of the sulfonyl bound to Na^+ have increased (by~0.022 Å) to 1.4809 Å and the free S=O bonds have decreased (by 0.012–0.013 Å) to 1.4506 Å. The >*C*=*O* bond lengths of the camphor group have increased by~0.01 Å upon metal binding.

3.3. Effect of Na^+ binding on the electronic distribution

Natural Bond Orbital (NBO) analysis was performed on urea in both free and bound form to see the change in atomic charges upon Na^+ binding (see Fig. 4 for atom label).

As can be seen from Table 2, charges on both sulfonyl and carbonyl oxygen decreased by~0.1 e and ~0.14 e, respectively. This implies electron transfer from catalyst to metal and results in a decrease in charge on Na atom (see Table 2). The charge on the C24 atom of the urea carbonyl has increased by~0.02 e, whereas on sulfur atoms have decreased by ~0.01 e. Both nitrogen atoms have gained charge (~0.01 e) as a result of Na^+ binding. NBO analysis reveals that the occupancy of $\pi^*(C{=}O)$ of urea increases upon Na^+ binding by~ 0.1 e. A gain in electron population in the anti-bonding orbital implies weakening of the bond [46]. This is reflected in the elongation of bond length (see Table 1) and a decrease in wavenumber of the corresponding stretching frequency (see next section). The population of σ(S–O) orbital bound to Na^+ decreased by~0.02 e which is in agreement with the increment of the corresponding bond lengths (Table 1). The decrease of C–N bond length can be attributed to the loss of electron population in the σ^* (C–N) orbital. The increased population of σ^* (N–H) orbitals causes the two N–H bonds to lengthen.

3.4. Effect of Na^+ binding on vibrational frequencies

Figs. 5 and 6 show the IR and Raman spectra of the catalyst, $NaBPh_4$, and the complex. A comparison of vibrational frequencies is made between the monomer of the urea catalyst and its bound form with sodium. Table 3 summarizes the calculated and observed frequencies, as well as assignments of modes that are sensitive to Na^+ binding.

A comparison of the IR spectrum of the free and sodium bound ureas shows a clear red-shift of the NH stretching frequency from 3268 cm^{-1} to 3221 cm^{-1} upon Na^+ binding. In theoretical calculations the shift is around 173 cm^{-1}. The disagreement in the absolute value may be due to the fact that the calculated value of urea catalyst is overestimated. However, the trend of shift could be well reproduced in calculation and this is attributed to the increase in length of the N–H bond (see Table 1). Upon Na^+ binding a net positive charge is induced in the complex, resulting in a decrease in the electron localization on nitrogen and a weakening of the N–H bond [47]. The other N–H frequency which appears at 3169 cm^{-1} in urea catalyst could not be detected in the complex form because of the weak intensity. The stretching frequencies of the keto carbonyl of the camphor group which are seen at 1734 and 1747 cm^{-1} in the free urea have shifted to 1730 and 1745 cm^{-1}, respectively in the complex. Unlike in the case of dimer, calculation on monomer produces only one peak at 1760 cm^{-1} which shifts to 1722 cm^{-1} after Na^+ binding. In Raman, this mode shifts by 7 cm^{-1} to lower wavenumber, while the predicted shift is 28 cm^{-1}. These shifts are in good agreement with the increase in >C=O bond length (see Table 1) in the complex. The increase in bond length can be attributed to the closeness of the carbonyl group to the N–H bond. It is to be mentioned, that the shift is overestimated in our calculation. In IR, the mode assigned as ν(>C=O) of urea at 1706 cm^{-1} disappeared on complexation and shifted to the O=H bending region of water (~1600 cm^{-1}) in the complex. By fitting Lorentzian curves in that region for both the catalyst and complex, we found a new mode at around 1599 cm^{-1} which was assigned to >C=O stretching of urea. The shift of 107 cm^{-1} is very close to the theoretically predicted value of 102 cm^{-1}. In Raman, the ν(C=O) mode of catalyst disappears in the complex form. The predicted mode at 1610 cm^{-1} could not be detected in the complex spectrum because of the appearance of strong phenyl ring modes of the $NaBPh_4$ in that region. The decrease in >*C*=*O* stretching frequency is reflected in the lengthening of the >*C*=*O* bond distance (Table 1) which is also supported by our NBO calculation (which shows increase in the population in anti-bonding orbital). The >*C*=*O* stretching frequency is known to red-shift upon metal binding and the amount of shift reflects the nature of the bond (more sensitive to ionic than covalent bond) [48,49]. The shifts observed in our case indicates that the metal–oxygen bond is predominantly ionic in nature. For the SO_2 group symmetric and antisymmetric stretching which appear at 1139 and 1344 cm^{-1} in IR spectrum of urea catalyst are

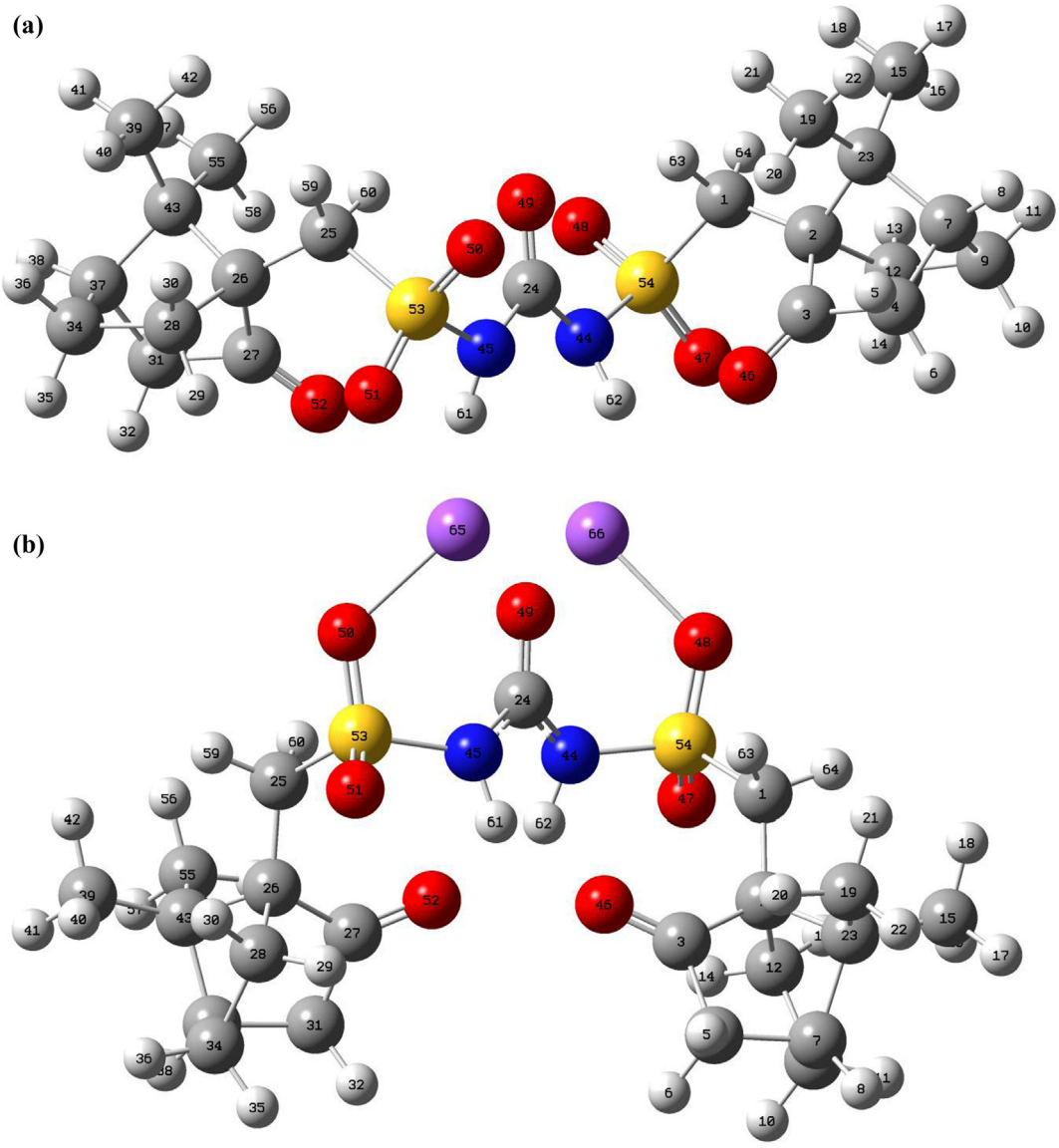

Fig. 4. The optimized monomer structure of urea in its free (a) and Na^+ bound (b) form. Color representation: white-hydrogen, gray-carbon, red-oxygen, blue-nitrogen, yellow-sulfur and violet-sodium. (For interpretation of the references to colour in this figure legend, the reader is referred to the web version of this article.)

down-shifted to 1135 and 1340 cm^{-1} in the complex form. The shift of 4 cm^{-1} of both the modes is in accordance with the predicted down-shift of 10 and 9 cm^{-1} respectively (see Table 3). In the Raman spectrum, the SO_2 anti-symmetric stretch is down-shifted by 13 cm^{-1}, the predicted value being 5 cm^{-1}. Symmetric SO_2 stretching is weak and falls in the region where contribution from counter-ion (BPh_4^-) occurs. Thus, we could not detect any shift of this mode in the complex. As can be seen from the optimized geometries, the S═O bond bound to Na^+ is lengthened, whereas

Table 1
Optimized bond lengths of the urea catalyst in its free and Na^+ bound form.

Geometrical parameter	Urea catalyst	Complex	Difference
Distance (Å)			
C24–O49	1.2209	1.2537	0.0328
C24–N45	1.3889	1.3769	−0.0120
C24–N44	1.3919	1.3769	−0.0150
N45–H61	1.0151	1.0268	0.0117
N44–H62	1.0154	1.0268	0.0114
S53–O50	1.4585	1.4809	0.0224
S53–O51	1.4630	1.4506	−0.0124
S54–O48	1.4588	1.4809	0.0221
S54–O47	1.4636	1.4506	−0.013
C27–O52	1.2134	1.2225	0.0091
C3–O46	1.2136	1.2225	0.0089

Table 2
Atomic charges (e) by NBO analysis on urea catalyst and complex.

	Urea catalyst	Complex	Difference
C 24	0.832	0.850	0.018
N 44	−0.923	−0.914	0.009
N 45	−0.922	−0.914	0.008
S 53	2.343	2.336	−0.007
S 54	2.346	2.336	−0.010
O 48	−0.923	−1.024	−0.101
O 49	−0.634	−0.773	−0.139
O 50	−0.926	−1.024	−0.098
Na 65		0.935	
Na 66		0.935	

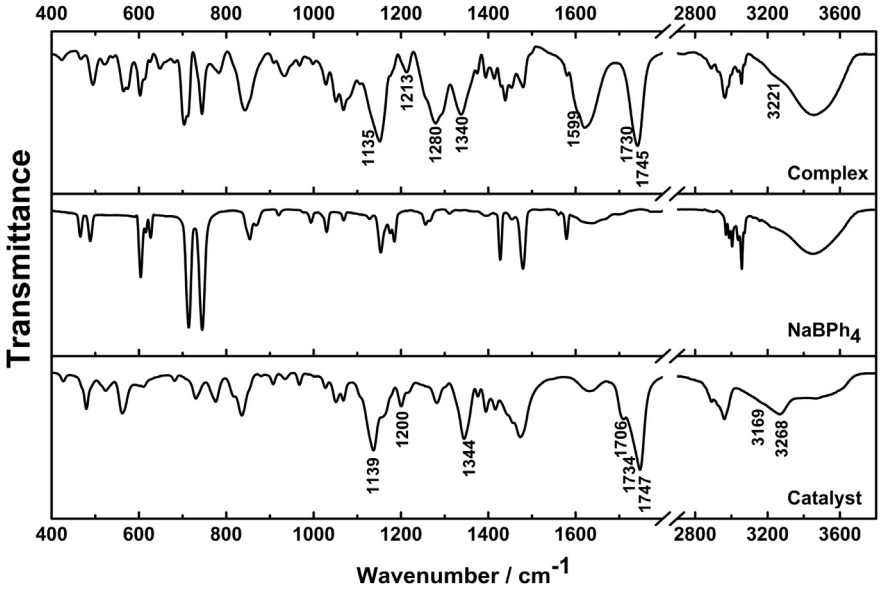

Fig. 5. The experimental IR spectra of urea catalyst, $NaBPh_4$, and complex.

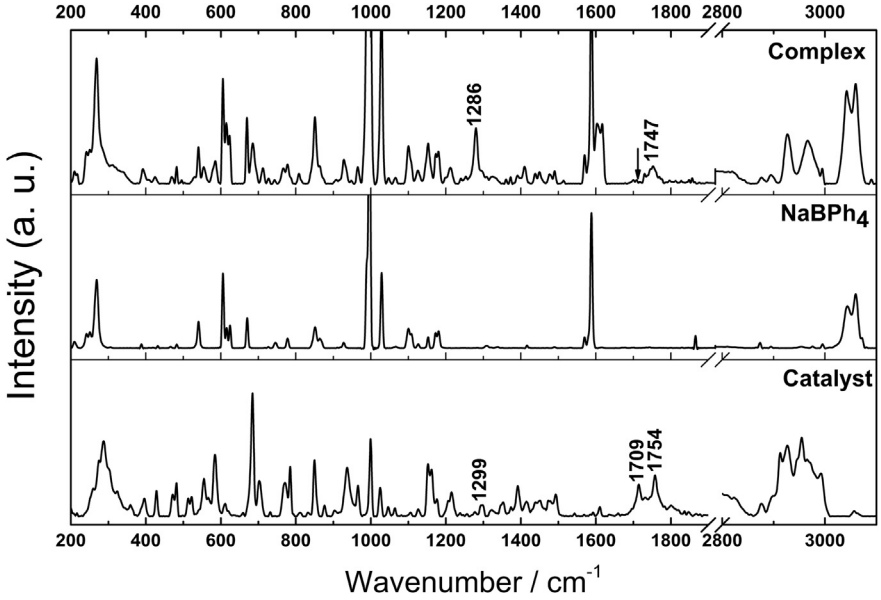

Fig. 6. The experimental Raman spectra of urea catalyst, $NaBPh_4$, and complex.

other S═O bond is shortened (see Table 1) in the SO_2 group. In the bound form, S═O stretching vibrations are mainly due to the contribution from the Na^+ bound S═O, as viewed by GaussView [50] visualization program. As this bond length increases upon metal binding, the decrease in wavenumber is expected. Decrease of the wavenumbers for both SO_2 vibrations were observed in metal saccharinates compared to saccharine compounds [48]. The C–N stretching vibration increased by 13 cm^{-1} upon complexation in the IR spectrum. This is in good agreement with the calculated value of 6 cm^{-1}. A slight decrease in C–N bond length accounts for this increase in wavenumber which corroborates with the NBO calculations. Decrease in the C–N bond length of saccharine was also observed by Jovanovski et al. [51] in metal-bound saccharinates. The observed changes in the infrared and Raman spectra upon complexation correlate with the DFT calculations. Mismatch between the theoretical and experimental value could most likely be due to the fact that in the calculation we considered a single molecule in gas phase. This overlooks the intermolecular interactions present in real system. The calculation could be possibly improved by the inclusion of the counter anion (tetraphenylborate), whose relative position with respect to the urea is not known experimentally. As a control, we have also calculated the infrared spectra for other possible conformations (see SI, Fig. 1) using same level of theory (see supporting information). The changes obtained with these calculations were not in agreement with the experimentally observed changes.

3.5. Conformational changes due to sodium binding

The conformation of the free and complexed urea were analyzed

Table 3
Selected vibrational frequencies (cm^{-1}) of the urea catalyst and the complex sensitive to the Na^+ binding.

Urea catalyst		Assignments, PED (%)	Complex		Assignments, PED (%)
Calculated	Observed		Calculated	Observed	
IR					
3452	3268	ν(N–H) (100)	3279	3221	ν(N–H) (99)
3444	3169	ν(N–H) (100)	3262	–	ν(N–H) (100)
1760	1734, 1747	ν(C=O) Cp (83)	1722	1730, 1745	ν(C=O) Cp (90)
1712	1706	ν(C=O) U (80)	1610	1599	ν(C=O) U (73), β(HNC) (18)
1303	1344	ν_{as}(S=O) (58)	1294	1340	ν_{as}(S=O) (69)
1163	1200	ν(C=N) (20)	1169	1213	ν(C–N) (27), β(HNC) (10)
1079	1139	ν_s(S=O) (33), β(HCC) (16)	1069	1135	ν_s(S=O) (77)
Raman					
1760	1754	ν(C=O) Cp (83)	1732	1747	ν(C=O) Cp (90)
1712	1709	ν(C=O) U (80)	1610	~1600	ν(C=O) U (73), β(HNC) (18)
1290	1299	ν_{as}(S=O) (26), Γ(HCCC) (12)	1285	1286	ν_{as}(S=O) (67)

Abbreviations: ν – stretching; β – in plane bending; Γ – torsion.
Cp – Camphor; U – Urea.
Subscripts: s-symmetric; as-antisymmetric.

using their simulated structures. Here we have focused on the differences in the dihedral angles between the carbonyl and sulfonyl groups of the free and complexed urea. In the free catalyst, the dihedral angle between the carbonyl group and one of the sulfonyl oxygens (O51 and O47) in each of the sulfonyl group are 168.5° and 168.3°. Upon sodium complexation both these angles shift to 120.8°. The other sulfonyl oxygens (O50 and O48) are in gauche-like orientation in the free urea (55.1° in each case). Whereas, in the sodium-complex this angle is 4.4°, which is a shift of 50.7° from the uncomplexed form. This makes the S53–O50 and C24–O49 bonds almost coplanar. Each of the camphor group is also in gauche-like conformation with respect to the urea carbonyl (51.7° and 51.3°) in the unbound catalyst. In the complex, these angles are seen to be 109.7° for both. This is a shift of ~58° which places the chiral camphonyl group near the urea hydrogens. This should enhance the selectivity for the Friedel–Crafts reaction by blocking one of the faces of β-nitro styrene when it is bound to the catalyst [11].

4. Conclusions

In summary, we have assigned the bands appearing in the IR and Raman spectra of the bis-camphorsulfonyl urea with the help of DFT calculation. For the free urea, a dimeric structure was considered and we obtained good agreement with the experimental value. For the sodium complex, theoretical calculations were performed by considering a monomer structure and the corresponding Raman and IR spectra were simulated. Our calculations support the idea that the sodium cation binds to the sulfonyl and urea carbonyl groups. The trends observed in experimental vibrational spectra are qualitatively reproduced in our calculation. This helped us in clearly explaining the changes in the stretching frequencies of sulfonyl, carbonyl, C–N, and N–H groups. NBO calculation reveals the electronic redistribution upon Na^+ binding. Overall, the binding of sodium results in a change in a new conformation where the camphor groups are closer to the hydrogen bond donors. This enhances the enantioselectivity of the Friedel–Crafts reaction. Furthermore, the spectra of the complex form together with the assignments would serve as a reference for studying binding mechanisms of different substrates to this catalyst.

Acknowledgments

The authors thank JNCASR and Department of Science and Technology, Ministry of Science and Technology for funding. P.P.K. and A.K.C. thank Council of Scientific and Industrial Researc for predoctoral research fellowships.

Appendix A. Supplementary data

Supplementary data related to this article can be found at http://dx.doi.org/10.1016/j.molstruc.2015.08.029.

References

[1] A.G. Doyle, E.N. Jacobsen, Small-molecule h-bond donors in asymmetric catalysis, Chem. Rev. 107 (12) (2007) 5713–5743.
[2] M.S. Taylor, E.N. Jacobsen, Asymmetric catalysis by chiral hydrogen-bond donors, Angew. Chem. Int. Ed. 45 (10) (2006) 1520–1543.
[3] S.J. Connon, Organocatalysis mediated by (Thio) urea derivatives, Chem. A Eur. J. 12 (21) (2006) 5418–5427.
[4] P.M. Pihko, Activation of carbonyl compounds by double hydrogen bonding: an emerging tool in asymmetric catalysis, Angew. Chem. Int. Ed. 43 (16) (2004) 2062–2064.
[5] S.J. Miller, In search of peptide-based catalysts for asymmetric organic synthesis, Acc. Chem. Res. 37 (8) (2004) 601–610.
[6] P.R. Schreiner, Metal-free organocatalysis through explicit hydrogen bonding interactions, Chem. Soc. Rev. 32 (5) (2003) 289–296.
[7] E.R. Jarvo, S.J. Miller, Amino acids and peptides as asymmetric organocatalysts, Tetrahedron 58 (13) (2002) 2481–2495.
[8] G. Jakab, C. Tancon, Z. Zhang, K.M. Lippert, P.R. Schreiner, (Thio) urea organocatalyst equilibrium acidities in DMSO, Org. Lett. 14 (7) (2012) 1724–1727.
[9] K.H. Jensen, M.S. Sigman, Evaluation of catalyst acidity and substrate electronic effects in a hydrogen bond-catalyzed enantioselective reaction, J. Org. Chem. 75 (21) (2010) 7194–7201.
[10] K.H. Jensen, M. Sigman, Systematically probing the effect of catalyst acidity in a hydrogen-bond-catalyzed enantioselective reaction, Angew. Chem. Int. Ed. 46 (25) (2007) 4748–4750, http://dx.doi.org/10.1002/anie.200700298. http://dx.doi.org/10.1002/anie.200700298.
[11] A.K. Chittoory, G. Kumari, S. Mohapatra, P.P. Kundu, T.K. Maji, C. Narayana, S. Rajaram, Conformational change in a urea catalyst induced by sodium cation and its effect on enantioselectivity of a friedel-crafts reaction, Tetrahedron 70 (21) (2014) 3459–3465. http://dx.doi.org/10.1016/j.tet.2014.03.068. http://www.sciencedirect.com/science/article/pii/S0040402014004165.
[12] A.G. Schafer, J.M. Wieting, A.E. Mattson, Silanediols: a new class of hydrogen bond donor catalysts, Org. Lett. 13 (19) (2011) 5228–5231.
[13] Y.-F. Sheng, Q. Gu, A.-J. Zhang, S.-L. You, Chiral bronsted acid-catalyzed asymmetric friedel- crafts alkylation of pyrroles with nitroolefins, J. Org. Chem. 74 (17) (2009) 6899–6901.
[14] M. Ganesh, D. Seidel, Catalytic enantioselective additions of indoles to nitroalkenes, J. Am. Chem. Soc. 130 (49) (2008) 16464–16465.
[15] J. Itoh, K. Fuchibe, T. Akiyama, Chiral phosphoric acid catalyzed enantioselective friedel–crafts alkylation of indoles with nitroalkenes: cooperative effect of 3 å molecular sieves, Angew. Chem. Int. Ed. 47 (21) (2008) 4016–4018.
[16] E.M. Fleming, T. McCabe, S.J. Connon, Novel axially chiral bis-arylthiourea-based organocatalysts for asymmetric friedel–crafts type reactions, Tetrahedron Lett. 47 (39) (2006) 7037–7042.
[17] R.P. Herrera, V. Sgarzani, L. Bernardi, A. Ricci, Catalytic enantioselective friedel–crafts alkylation of indoles with nitroalkenes by using a simple thiourea organocatalyst, Angew. Chem. Int. Ed. 44 (40) (2005) 6576–6579.
[18] W. Zhuang, R.G. Hazell, K.A. Jørgensen, Enantioselective friedel–crafts type addition of indoles to nitro-olefins using a chiral hydrogen-bonding

catalyst–synthesis of optically active tetrahydro-β-carbolines, Org. Biomol. Chem. 3 (14) (2005) 2566–2571.
[19] G. Dessole, R.P. Herrera, A. Ricci, H-bonding organocatalysed friedel-crafts alkylation of aromatic and heteroaromatic systems with nitroolefins, Synlett 2004 (13) (2004) 2374–2378.
[20] G.P. Kumar, C. Narayana, Adapting a fluorescence microscope to perform surface enhanced, Curr. Sci. 93 (6) (2007) 778–781.
[21] M.J. Frisch, G.W. Trucks, H.B. Schlegel, G.E. Scuseria, M.A. Robb, J.R. Cheeseman, G. Scalmani, V. Barone, B. Mennucci, G.A. Petersson, H. Nakatsuji, M. Caricato, X. Li, H.P. Hratchian, A.F. Izmaylov, J. Bloino, G. Zheng, J.L. Sonnenberg, M. Hada, M. Ehara, K. Toyota, R. Fukuda, J. Hasegawa, M. Ishida, T. Nakajima, Y. Honda, O. Kitao, H. Nakai, T. Vreven, J.A. Montgomery Jr., J.E. Peralta, F. Ogliaro, M. Bearpark, J.J. Heyd, E. Brothers, K.N. Kudin, V.N. Staroverov, R. Kobayashi, J. Normand, K. Raghavachari, A. Rendell, J.C. Burant, S.S. Iyengar, J. Tomasi, M. Cossi, N. Rega, J.M. Millam, M. Klene, J.E. Knox, J.B. Cross, V. Bakken, C. Adamo, J. Jaramillo, R. Gomperts, R.E. Stratmann, O. Yazyev, A.J. Austin, R. Cammi, C. Pomelli, J.W. Ochterski, R.L. Martin, K. Morokuma, V.G. Zakrzewski, G.A. Voth, P. Salvador, J.J. Dannenberg, S. Dapprich, A.D. Daniels, J.B. Farkas, J.V. Foresman, J. Ortiz, D.J. Cioslowski, Fox, Gaussian 09 Revision D.01, gaussian Inc, Wallingford CT, 2009.
[22] A.D. Becke, Density-functional thermochemistry. III. The role of exact exchange, J. Chem. Phys. 98 (7) (1993) 5648–5652, http://dx.doi.org/10.1063/1.464913. http://link.aip.org/link/?JCP/98/5648/1.
[23] C. Lee, W. Yang, R.G. Parr, Development of the colle-salvetti correlation-energy formula into a functional of the electron density, Phys. Rev. B 37 (1988) 785–789, http://dx.doi.org/10.1103/PhysRevB.37.785. http://link.aps.org/doi/10.1103/PhysRevB.37.785.
[24] Nist computational chemistry comparison and benchmark database (cccbdb), nist standard reference database number 101, release 16a, august 2013, editor: Johnson iii, russell d; http://cccbdb.nist.gov/.
[25] P. Polavarapu, Ab initio vibrational Raman and Raman optical activity spectra, J. Phys. Chem. 94 (21) (1990) 8106–8112.
[26] V. Krishnakumar, G. Keresztury, T. Sundius, R. Ramasamy, Simulation of IR and Raman spectra based on scaled DFT force fields: a case study of 2-(methylthio) benzonitrile, with emphasis on band assignment, J. Mol. Struct. 702 (1) (2004) 9–21.
[27] S.D. Williams, T.J. Johnson, T.P. Gibbons, C.L. Kitchens, Relative raman intensities in c6h6, c6d6, and c6f6: a comparison of different computational methods, Theor. Chem. Acc. 117 (2) (2007) 283–290.
[28] M.H. Jamróz, Vibrational energy distribution analysis veda 4, (Warsaw).
[29] E.D. Glendening, A.E. Reed, J.E. Carpenter, F.Weinhold, NBO Version 3.1.
[30] D.W. Mayo, F.A. Miller, R.W. Hannah, Course Notes on the Interpretation of Infrared and Raman Spectra, John Wiley & Sons, 2004.
[31] J.R.A. Moreno, F.P. Ureña, J.J.L. González, Chiral terpenes in different matrices: R-(+)-camphor studied by ir-raman-vcd spectroscopies and quantum chemical calculations, Asian J. Spectrosc. 14 (1–2) (2010) 1–21.
[32] J.R.A. Moreno, F.P. Ureña, J.J.L. González, Chiral terpenes in different phases: R-(-)-camphorquinone studied by ir–raman–vcd spectroscopies and theoretical calculations, Struct. Chem. 22 (1) (2011) 67–76.
[33] H. Ciurla, J. Michalski, J. Hanuza, M. Mczka, T. Talik, Z. Talik, Molecular structure, IR and Raman spectra as well as DFT chemical calculations for alkylaminoacetylureas: vibrational characteristics of dicarbonylimide bridge, Spectrochimica Acta Part A Mol. Biomol. Spectrosc. 64 (1) (2006) 34–46. http://dx.doi.org/10.1016/j.saa.2005.06.035. http://www.sciencedirect.com/science/article/pii/S1386142505003355.
[34] C. Meganathan, S. Sebastian, I. Sivanesan, K.W. Lee, B.R. Jeong, H. Oturak, S. Sudha, N. Sundaraganesan, Structural, vibrational (FT-IR and FT-Raman) and uv–vis spectral analysis of 1-phenyl-3-(1, 2, 3-thiadiazol-5-yl) urea by DFT method, Spectrochimica Acta Part A Mol. Biomol. Spectrosc. 95 (2012) 331–340.
[35] N.P. Roeges, A Guide to the Complete Interpretation of Infrared Spectra of Organic Structures, Wiley, 1994.
[36] F.R. Dollish, W.G. Fateley, F.F. Bentley, Characteristic Raman Frequencies of Organic Compounds, Vol. 27, Wiley, New York, 1974.
[37] A. Hangan, A. Bodoki, L. Oprean, G. Alzuet, M. Liu-Gonzlez, J. Borrs, Synthesis, crystallographic and spectroscopic characterization and magnetic properties of dimer and monomer ternary copper(ii) complexes with sulfonamide derivatives and 1,10-phenanthroline. nuclease activity by the oxidative mechanism, Polyhedron 29 (4) (2010) 1305–1313. http://dx.doi.org/10.1016/j.poly.2009.12.030. http://www.sciencedirect.com/science/article/pii/S0277538710000124.
[38] Z.H. Chohan, M.H. Youssoufi, A. Jarrahpour, T.B. Hadda, Identification of antibacterial and antifungal pharmacophore sites for potent bacteria and fungi inhibition: indolenyl sulfonamide derivatives, Eur. J. Med. Chem. 45 (3) (2010) 1189–1199. http://dx.doi.org/10.1016/j.ejmech.2009.11.029. http://www.sciencedirect.com/science/article/pii/S0223523409005996.
[39] H. Alyar, A. Ünal, N. Özbek, S. Alyar, N. Karacan, Conformational analysis, vibrational and nmr spectroscopic study of the methanesulfonamide-n, n-1, 2-ethanediylbis, Spectrochimica Acta Part A Mol. Biomol. Spectrosc. 91 (2012) 39–47.
[40] S. Kudoh, M. Takayanagi, M. Nakata, T. Ishibashi, M. Tasumi, Infrared-induced rotational isomerization of 1, 2-ethanediamine in argon matrices and conformational analysis by DFT calculation, J. Mol. Struct. 479 (1) (1999) 41–52.
[41] Y.-l Lam, H. Huang, Rotational isomerism in 1, 2-diaminoethane, 1, 2-bis (dimethylamino) ethane and 1, 2-bis (diethylamino) ethane, J. Mol. Struct. 412 (1–2) (1997) 141–152.
[42] L. Batista de Carvalho, L. Lourenco, M. Marques, Conformational study of 1, 2-diaminoethane by combined ab initio MO calculations and Raman spectroscopy, J. Mol. Struct. 482 (1999) 639–646.
[43] A. Chandran, Y.S. Mary, H.T. Varghese, C.Y. Panicker, P. Pazdera, G. Rajendran, FT-IR, FT-Raman spectroscopy and computational study of (e)-4-((anthracen-9-ylmethylene) amino)-n-carbamimidoylbenzene sulfonamide, Spectrochimica Acta Part A Mol. Biomol. Spectrosc. 79 (5) (2011) 1584–1592.
[44] C. Baraldi, M. Gamberini, A. Tinti, F. Palazzoli, V. Ferioli, Vibrational study of acetazolamide polymorphism, J. Mol. Struct. 918 (1) (2009) 88–96.
[45] P.P. Kundu, G. Pavan Kumar, K. Mantelingu, T.K. Kundu, C. Narayana, Raman and surface enhanced Raman spectroscopic studies of specific, small molecule activator of histone acetyltransferase p300, J. Mol. Struct. 999 (1) (2011) 10–15.
[46] A.E. Reed, L.A. Curtiss, F. Weinhold, Intermolecular interactions from a natural bond orbital, donor-acceptor viewpoint, Chem. Rev. 88 (6) (1988) 899–926.
[47] R.N. Allen, M. Shukla, J.V. Burda, J. Leszczynski, Theoretical study of interaction of urate with li⁺, na⁺, k⁺, be²⁺, mg²⁺, and ca²⁺ metal cations, J. Phys. Chem. A 110 (18) (2006) 6139–6144.
[48] G. Jovanovski, S. Tančeva, B. Šoptrajanov, The SO_2 stretching vibrations in some metal saccharinates: spectra-structure correlations, Spectrosc. Lett. 28 (7) (1995) 1095–1109.
[49] P. Naumov, G. Jovanovski, Vibrational study and spectra-structure correlations in ammonium saccharinate: comparison with the alkali saccharinates, Spectrochimica Acta Part A Mol. Biomol. Spectrosc. 56 (7) (2000) 1305–1318.
[50] R. Dennington, T. Keith, J. Millam, Gaussview Version 5, semichem Inc, Shawnee Mission KS, 2009.
[51] G. Jovanovski, B. Šoptrajanov, Bonding of the carbonyl group in metal saccharinates: correlation with the infrared spectra, J. Mol. Struct. 174 (1988) 467–472.